

Ionic-liquid-like copolymer stabilized nanocatalysts in ionic liquids: II. Rhodium-catalyzed hydrogenation of arenes

Chen Zhao^a, Han-zhi Wang^a, Ning Yan^a, Chao-xian Xiao^a, Xin-dong Mu^a, Paul J. Dyson^{b,*},
Yuan Kou^{a,*}

^a PKU Green Chemistry Center, Beijing National Laboratory for Molecular Sciences, College of Chemistry and Molecular Engineering, Peking University, Beijing 100871, China

^b Institut des Sciences et Ingénierie Chimiques, Ecole Polytechnique Fédérale de Lausanne (EPFL), CH-1015 Lausanne, Switzerland

Received 20 March 2007; revised 18 May 2007; accepted 22 May 2007

Available online 28 June 2007

Abstract

Rhodium nanoparticles stabilized by the ionic-liquid-like copolymer poly[(*N*-vinyl-2-pyrrolidone)-*co*-(1-vinyl-3-butylimidazolium chloride)] were used to catalyze the hydrogenation of benzene and other arenes in ILs. The nanoparticle catalysts can endure forcing conditions (75 °C, 40 bar H₂), resulting in high reaction rates and high conversions compared with other nanoparticles that operate in ILs. The hydrogenation of benzene attained record total turnovers of 20,000, and the products were easily separated without being contaminated by the catalysts. Other substrates, including alkyl-substituted arenes, phenol, 4-*n*-propylphenol, 4-methoxyphenol, and phenyl-methanol, were studied and in most cases were found to afford partially hydrogenated products in addition to cyclohexanes. In-depth investigations on reaction optimization, including characterization of copolymers, transmission electron microscopy, and an infrared spectroscopic study of nanocatalysts, were also undertaken. © 2007 Elsevier Inc. All rights reserved.

Keywords: Rhodium; Nanoparticles; Hydrogenation; Biphasic catalysis; Ionic liquids; Lignins; Copolymer

1. Introduction

Soluble nanoparticle catalysts with unique properties have aroused increasing interest in recent years due to their potentially high catalytic efficiency [1,2]. Unlike their counterparts restricted on solid surfaces, soluble nanoparticles with their rotational freedom and spherically symmetrical geometry are, at least in principle, more active [3].

Ionic liquids (ILs) provide the opportunity to combine the advantages of both homogeneous and heterogeneous processes in a single system [3,4]. Immobilization of nanoparticles by “supporting” them in an IL rather than on a surface preserves the rotationally free catalytic centers, in keeping with soluble nanoparticle systems. Moreover, the low interfacial tension and

structural organization of ILs are believed to be effective for preparing small nanoparticles and for controlling extended ordering of nanoscale structures [5]. In addition, evidence has been found relating to the fact that imidazolium-based ILs are good stabilizers for transition-metal nanoparticles [6].

Generally, the most pertinent problem encountered in soluble nanoparticle applications is the need to stabilize the particles against aggregation or agglomeration, which tends to be done by adding stabilizers. Examples of stabilizers used in conjunction with catalytically active soluble nanoparticles include solvents [7,8], soluble polymers [9], quaternary ammonium salts [10], and polyoxoanions [11]. It must be kept in mind that very stable nanoparticles are not the ultimate aim in catalysis, because they are generally less active, due to “overprotection” of the catalytically active nanoparticle surface. In our previous communication, rhodium nanoparticles protected by “IL-like” copolymers were shown to catalyze benzene hydrogenation with a record of total turnover (TTO) of 20,000 [12],

* Corresponding authors. Faxes: +86 10 62751708, +41 21 693 98 85.
E-mail addresses: yuankou@pku.edu.cn (Y. Kou), paul.dyson@epfl.ch (P.J. Dyson).

demonstrating that an optimum balance between stability and reactivity to be a critical parameter.

The hydrogenation of benzene and arenes, which is accomplished using heterogeneous catalysts almost exclusively [13,14], molecular precatalysts immobilized on heterogeneous surfaces [15–17], supported nanoparticle [18], or soluble nanoparticle [19,20] systems, sometimes inadvertently derived from molecular precursors [21,22], represents an important industrial catalytic transformation, particularly for the production of cleaner-burning, low-aromatic diesel fuels [13]. The partial hydrogenation of arenes, which is far more difficult to realize, is equally important because it can help to simplify many multistage synthetic procedures and allow the use of alternative precursors [23]. The catalytic procedure for partial hydrogenation of arenes generally is not simple; for example, the selective hydrogenation of benzene to cyclohexene performed on an industrial scale involves a multiphase process using a ruthenium-based heterogeneous catalyst, which results in 90% conversion and 60% selectivity [24].

In an extension to our preliminary report on Rh nanoparticles that catalyze the hydrogenation of benzene in ILs with unprecedented lifetimes [12], we now describe their application to the hydrogenation of benzene and other arenes in greater detail. IL-like copolymers were evaluated in terms of composition and average molecular weight and compared with poly(*N*-vinyl-2-pyrrolidone) (PVP), a widely used protecting agent [9,25]. The hydrogenation of arene substrates with various alkyl and other substituents was then investigated, and activities were correlated to nanoparticle structure. Moreover, we found that these rhodium nanoparticles are highly active catalysts for the partial hydrogenation of arene substrates in ILs, with very high selectivity toward the monoene in some cases.

2. Experimental

2.1. Synthesis of copolymers

2.1.1. Synthesis of 1-vinyl-3-butylimidazolium chloride ([VBIM]Cl)

1-Vinylimidazole (5.00 g, 53 mmol) and butyl chloride (18.50 g, 200 mmol) were mixed and stirred vigorously at 70 °C for 24 h. The residual mixture was cooled to 0 °C, and then the upper liquid layer was removed by decantation. The residue was then washed with ethyl acetate (3 × 30 ml), evaporated under vacuum, and dried to yield a pale-yellow solid [VBIM]Cl (7.74 g, 75%).

¹H NMR δ (300 MHz, D₂O) 0.98 (t, J = 7.6, 3H, CH₃), 1.41 (m, 2H, CH₂), 1.95 (m, 2H, CH₂), 4.41 (t, J = 7.6, 2H, CH₂), 5.39 (dd, J = 8.7, 3.0, 1H, CH), 6.01 (dd, J = 14.7, 2.7, 1H, CH), 7.55 (dd, J = 14.7, 8.7, 2H, CH₂), 7.88 (s, 1H, NH), 11.35 (s, 1H, NH) ppm.

¹³C NMR δ (75 MHz, D₂O) 13.40, 19.41, 32.00, 50.06, 101.82, 118.92, 122.35, 128.41, 136.87 ppm.

Anal. Calcd. for C₉H₁₅N₂Cl: C, 57.90; H, 8.10; N, 15.01. Found: C, 57.81; H, 8.02; N, 15.10.

HRMS Calcd. for C₉H₁₅N₂⁺: 151.1230. Found: 151.1227.

2.1.2. Synthesis of 1-vinyl-3-ethylimidazolium bromide ([VEIM]Br)

1-Vinylimidazole (5.00 g, 53 mmol) was mixed with ethyl bromide (6.54 g, 60 mmol), and the mixture was stirred vigorously at 70 °C for 3 h. After reaction, the ethyl bromide was removed under vacuum at 60 °C for 2 h to afford a pale-yellow solid [VEIM]Br. Yield 9.80 g, 95%.

¹H NMR δ (300 MHz, D₂O) 1.35 (t, J = 7.6, 3H, CH₃), 4.10 (q, J = 7.6, 2H, CH₂), 5.24 (dd, J = 8.6, 2.4, 2H, CH₂), 5.62 (dd, J = 15.2, 2.4, 1H, CH), 6.96 (dd, J = 15.2, 8.6, 1H, CH), 7.30 (s, 1H, NH), 7.59 (s, 1H, NH).

¹³C NMR δ (75 MHz, D₂O) 16.61, 47.50, 111.44, 113.01, 121.66, 124.81, 130.57 ppm.

Anal. Calcd. for C₇H₁₁N₂Br: C, 41.40; H, 5.46; N, 13.79. Found: C, 41.47; H, 5.55; N, 13.95.

HRMS Calcd. for C₇H₁₁N₂⁺: 123.0917. Found: 123.0915.

2.1.3. Copolymerization

A mixture of *N*-vinyl-2-pyrrolidone (NVP) (0.5 g, 4.5 mmol), [VBIM]Cl (0.43 g, 2.3 mmol) or [VEIM]Br (0.46 g, 2.3 mmol), and 2,2'-azo-bis-isobutyronitrile (AIBN) (6.9 mg, 0.042 mmol) in methanol (5 ml, degassed by 3 freeze/thaw cycles) was stirred in a preheated oil bath at 60 °C for 16 h. The resulting solid was dissolved in methanol (5 ml) and precipitated in diethyl ether (500 ml). The residual monomers were removed by dialysis in distilled water for 24 h, and the solvent was removed under reduced pressure. Finally, the copolymers were dried under vacuum at room temperature. Yield ~0.8 g.

2.2. Preparation of Rh nanoparticles in ILs

Rhodium nanoparticles were prepared by reduction of RhCl₃ (1.6 × 10⁻⁵ mol) with H₂ in 1-butyl-3-methylimidazolium tetrafluoroborate ([BMIM][BF₄]) (6 ml) containing poly(NVP-co-VBIMCl) ([poly(NVP-co-VBIMCl)]/[Rh] = 5:1). Typically, the preparation was carried out in a 100 ml autoclave to afford a black solution after reduction at 60 °C and H₂ (40 bar) for 30 min.

2.3. Arene hydrogenation reactions

The arene (32 mmol) and Rh nanoparticle solution (6 ml, synthesized as described above) were placed in the autoclave. In a typical experiment, H₂ (40 bar) was introduced into the autoclave after the reactor was purged 3 times with H₂. The mixture was stirred at 800 rpm at 75 °C for 10 h, which afforded a two-phase system (the lower IL phase-containing catalysts and the upper organic phase). The upper layer was decanted and analyzed by GC, GC-MS, IR, and ¹H NMR spectroscopy.

2.4. Mercury poisoning experiments

2.4.1. Experiment 1. Hydrogenation without mercury

To a solution of [BMIM][BF₄] (6 ml) containing Rh nanoparticles (0.016 mmol Rh) and poly(NVP-co-VBIMCl) (0.08 mmol), benzene (2.5 g, 32 mmol) was added in a 100 ml

autoclave. The reactor was purged 3 times with H₂ and the reactor was pressurized to 40 bar. The mixture was reacted at 75 °C and stirred at 800 rpm for 8 h.

2.4.2. Experiment 2. Hydrogenation with addition of mercury

The reaction procedure was the same as described in experiment 1, except, the reaction was stopped when conversion reached 50% and mercury (3.21 g, 16 mmol, 1000 equiv.) was added to the autoclave. Then the mixture was stirred for 1 h under protection of nitrogen, the reactor was repressurized with H₂ (40 bar), and the reaction continued. A graph showing the effect of mercury poisoning experiments is given in Fig. S3.

2.5. Characterization

2.5.1. ICP measurements

Rhodium loss after catalytic reactions was measured by ICP. In this procedure, the product phase was mixed with 40 ml of aqua regia and refluxed at 100 °C for 18 h. The resulting solution was diluted to 50 ml with water and used for the ICP measurement (PROFILE SPEC, LEEMAN LABS, detection limit ~µg–mg/ml).

2.5.2. High-resolution transmission electron microscopy (HRTEM)

Transmission electron microscopic micrographs were recorded on a Hitachi H-9000 HRTEM at 300 keV. Rh nanoparticles immobilized in [BMIM][BF₄] were diluted in methanol. Samples were prepared by the dropwise addition of the Rh nanoparticle suspension onto Cu grids coated with holey carbon. More than 200 particles were counted to determine the size distribution.

2.5.3. Fourier-transform infrared spectroscopy (FTIR)

A flow of 1 bar CO was bubbled into [BMIM][BF₄] (1 ml) solution containing Rh nanoparticles for 2 h. The solution was then spread into a liquid film on KBr windows, and IR spectra were recorded immediately on a Bruker Tensor 27 Fourier-transform infrared spectrometer with a resolution of 1 cm⁻¹ at 20 °C.

3. Results and discussion

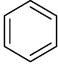
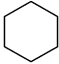
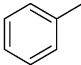
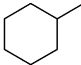
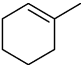
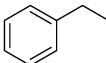
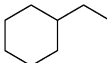
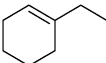
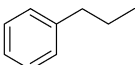
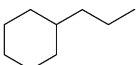
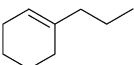
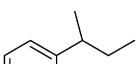
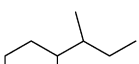
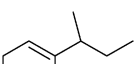
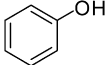
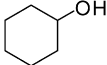
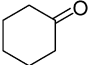
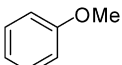
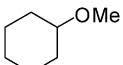
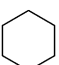
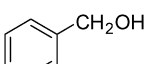
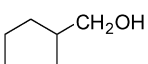
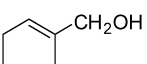
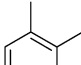
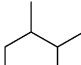
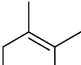
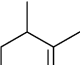
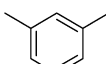
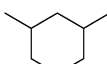
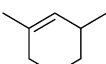
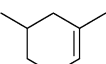
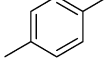
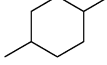
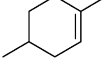
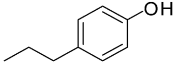
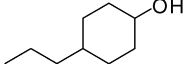
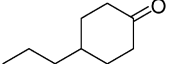
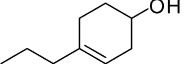
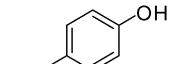
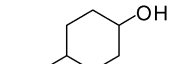
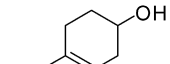
3.1. Hydrogenation of benzene and arene derivatives

As reported previously, the rhodium nanoparticles stabilized by an IL-like copolymer [poly(NVP-co-VBIMCl)] showed unprecedented lifetime and activity for benzene hydrogenation under relatively mild conditions with a TTO of 20,000 (from five recyclings of 4000 TTOs per batch) and TOFs exceeding 200 h⁻¹ [12]. It was shown that the Rh⁰ nanoparticles could be used at least 5 times without deterioration in activity (i.e., quantitative conversion under the conditions used) for benzene hydrogenation, demonstrating that the combination of ILs with IL-like stabilizers represents an excellent strategy for providing highly stable, catalytically active nanoparticles.

In an extension to this work, a series of nanoparticles stabilized by poly(NVP-co-VBIMCl) were evaluated as catalysts for benzene hydrogenation in ILs under various conditions (Table S1 in the supporting information). Various parameters were explored, including the nature of the metal, the IL used, and the preparation method of the nanoparticles. In this way, the activity of the nanoparticles was optimized. It was found that the Rh⁰ nanoparticles were considerably more active than the Ru⁰ and Pd⁰ nanoparticles in the ILs (Table S1, entries 1–11).

The rhodium nanoparticles protected by the IL-like copolymer were also found to be active catalysts in the hydrogenation of other arenes, and because these nanoparticles can endure comparative forcing conditions, faster reaction rates and higher conversions were obtained for the hydrogenation of arenes compared with those catalyzed by nanoparticles protected only by imidazolium ILs (see Table 1). Furthermore, the products could be separated from the IL (catalyst) phase by decantation, and loss of rhodium was below the detection limit of the ICP instrument (<1 µg/ml). The Rh nanoparticles immobilized in ILs are excellent catalysts for arene hydrogenation reactions irrespective of the presence of functional groups. In the present study, only arenes with oxygen-containing functional groups were examined, because these substrates correspond to model lignin compounds (the hydrogenation of lignins is important in paper production [26] and the production of fuels from biomass [27]). As described elsewhere [28], the TOF for benzene hydrogenation is higher than that of arenes under the same reaction conditions, with conversions and TOFs of alkyl derivatives decreasing with increasing size or number of substituents. This is believed to be due to a balance between the coordination properties of a particular arene (a prerequisite for hydrogenation) and electronic stabilization/destabilization of the aromatic character by the substituent groups, with the two effects often working against each other. The hydrogenolysis product observed from the hydrogenation of anisole is negligible under the given conditions ([substrate]/[rhodium] = 2000 mol/mol). Remarkably, whereas simple arene substrates yield the expected hydrogenated product with >99% selectivity, reduction of certain substrates results in the formation of significant quantities of partially hydrogenated products. (See Tables 2 and S2–S6 in supporting information for details of reaction optimization.) The unsaturated bond in the partially hydrogenated products is, as expected, stabilized by electron-donating substituents attached to the aromatic ring. Previously, it has been shown that substrates such as 1,2,4,5-tetramethylbenzene and anisole may be converted into their corresponding monoenes by Rh⁰ nanoparticles in aqueous phases [29,30]. In addition, partial hydrogenation of linear and cyclic dienes has previously been accomplished in IL biphasic systems using molecular catalysts [31–33] and soluble nanoparticles [7,8]. It was shown that the increased levels of partially hydrogenated products were due in part to the higher solubility of the diene relative to the monoene in the IL, which results in its spontaneous elimination from the catalyst phase [34]. Partial reduction of benzene also has been reported using nanoparticle catalysts in ILs [35,36]. Because far more active catalysts are required to hydrogenate arenes compared with alkenes, by virtue of the need to break the aromaticity,

Table 1
Hydrogenation^a of arenes by IL-like copolymer^b stabilized rhodium nanoparticles in [BMIM][BF₄]

Entry	Substrate	Conversion (%) ^c	Product ₁ (%) ^d	Product ₂ (%)	Product ₃ (%)	TOF ^e (h ⁻¹)
1		96	 100%			160
2		95	 >99%	 <1%		158
3		82	 >99%	 <1%		137
4		22	 81%	 19%		130
5		37	 62%	 38%		62
6		37	 71%	 29%		247
7		84	 >99%	 <1%		140
8		15	 74%	 26%		100
9		33	 68%	 16%	 16%	55
10		42	 88%	 6%	 6%	70
11		41	 90%	 10%		68
12		11	 32%	 49%	 19%	25
13 ^f		21	 71%	 29%		70

^a Conditions: 1.6×10^{-5} mol Rh in 6 ml [BMIM][BF₄], [S]/[Rh] = 2000, 40 atm H₂, 75 °C, stirred at 800 min⁻¹ for 12 h.

^b Poly(NVP-co-VBIMCl) ($M_n = 50,400$, $M_w = 75,300$), IL-copolymer/Rh = 5:1 (mol/mol).

^c Determined by GC analysis.

^d Product proportions.

^e TOF based on mole substrate conversion per total mol metal per hour during the first 10 h.

^f [S]/[Rh] = 1000.

Table 2
Characterization of copolymers^a

Entry	M_n^b	M_w^c	M_w/M_n
1	17,900	21,500	1.20
2	25,000	32,000	1.28
3	50,400	75,300	1.49

^a The concentration of NVP (mol%) in the poly(NVP-*co*-VBIMCl) is 57%, which was determined by NMR with an average molecular weight of the repeating unit of 143.6 g/mol.

^b Numeral-average molecular weight.

^c Weight-average molecular weight.

suppressing further hydrogenation is a considerable challenge and results in somewhat lower selectivity toward the partial hydrogenation product compared with dienes; for example, cyclohexadiene can be converted to cyclohexene with a selectivity of 96% with high conversion [31]. It is interesting to note that dienes are not observed, in keeping with the solubility effect described; that is, the dienes are soluble in the IL phase and thus

are hydrogenated further. Such solvent effects also influence the conversion and turnover frequency, because mass transport between the phases becomes important. It is noteworthy that whereas hydrogen gas solubility is low in ILs, the rate of mass transfer of hydrogen into ILs appears to be very fast [37] and is unlikely to be rate-limiting under the reaction conditions.

3.2. Characterization and influence of the copolymers

The method used to prepare the IL-like copolymers is illustrated in Scheme S1 in supporting information. Two IL-like copolymers, poly[NVP-*co*-VBIM]Cl and poly[NVP-*co*-VEIM]Br, and the homopolymer (poly[VBIM]Cl) (Figs. 1 and 2) were prepared for comparison purposes. The polymer concentration and ratio of [copolymer]/[Rh] (with the mol amount of polymer calculated by the amount of equivalent monomer) were 1.33×10^{-5} mol/ml and 5:1 mol/mol, respectively. The numeral-average molecular weight of the polymers

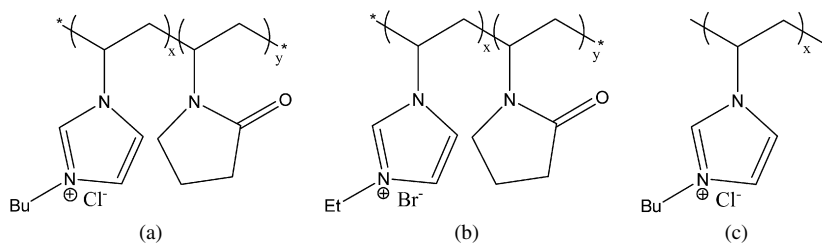


Fig. 1. Structure of (a) poly[(*N*-vinyl-2-pyrrolidone)-*co*-(1-vinyl-3-butylimidazolium chloride)], abbreviated as poly[NVP-*co*-VBIM]Cl; (b) poly[(*N*-vinyl-2-pyrrolidone)-*co*-(1-vinyl-3-ethylimidazolium bromide)], abbreviated as poly[NVP-*co*-VEIM]Br, (c) poly(1-vinyl-3-butylimidazolium chloride), abbreviated as poly[VBIM]Cl.

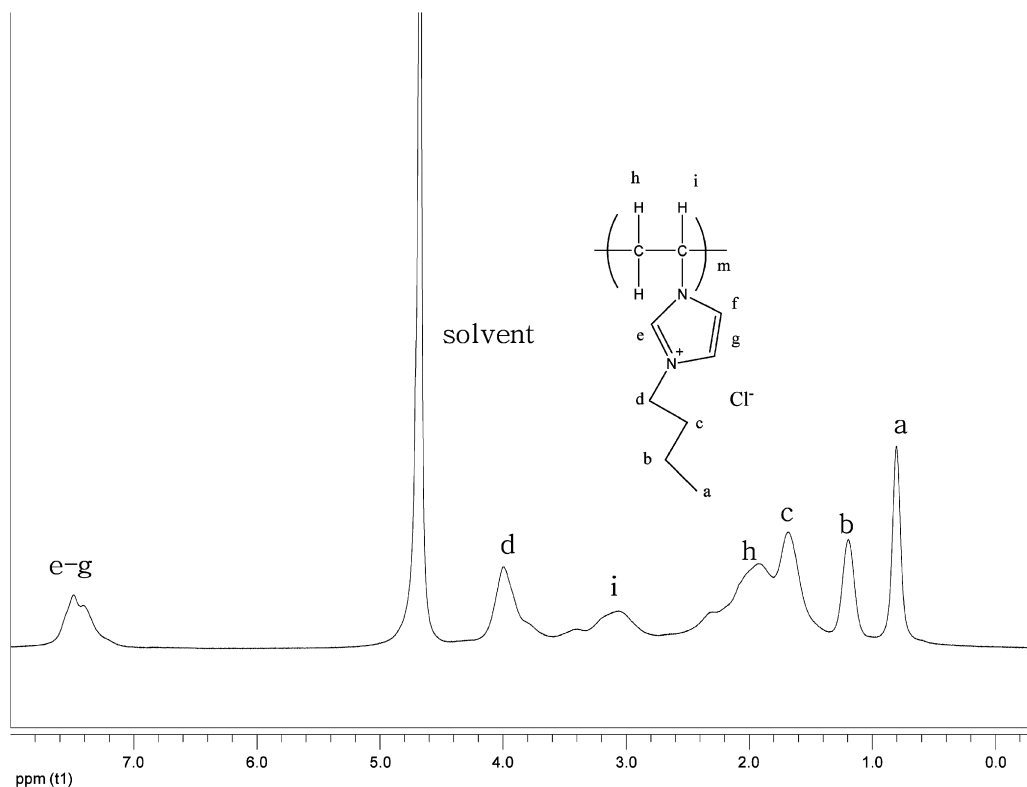


Fig. 2. ¹H NMR spectrum of poly[VBIM]Cl, spectra of poly[NVP-*co*-VBIM]Cl and poly[NVP-*co*-VEIM]Br are shown in Figs. S1 and S2. Solvent D₂O.

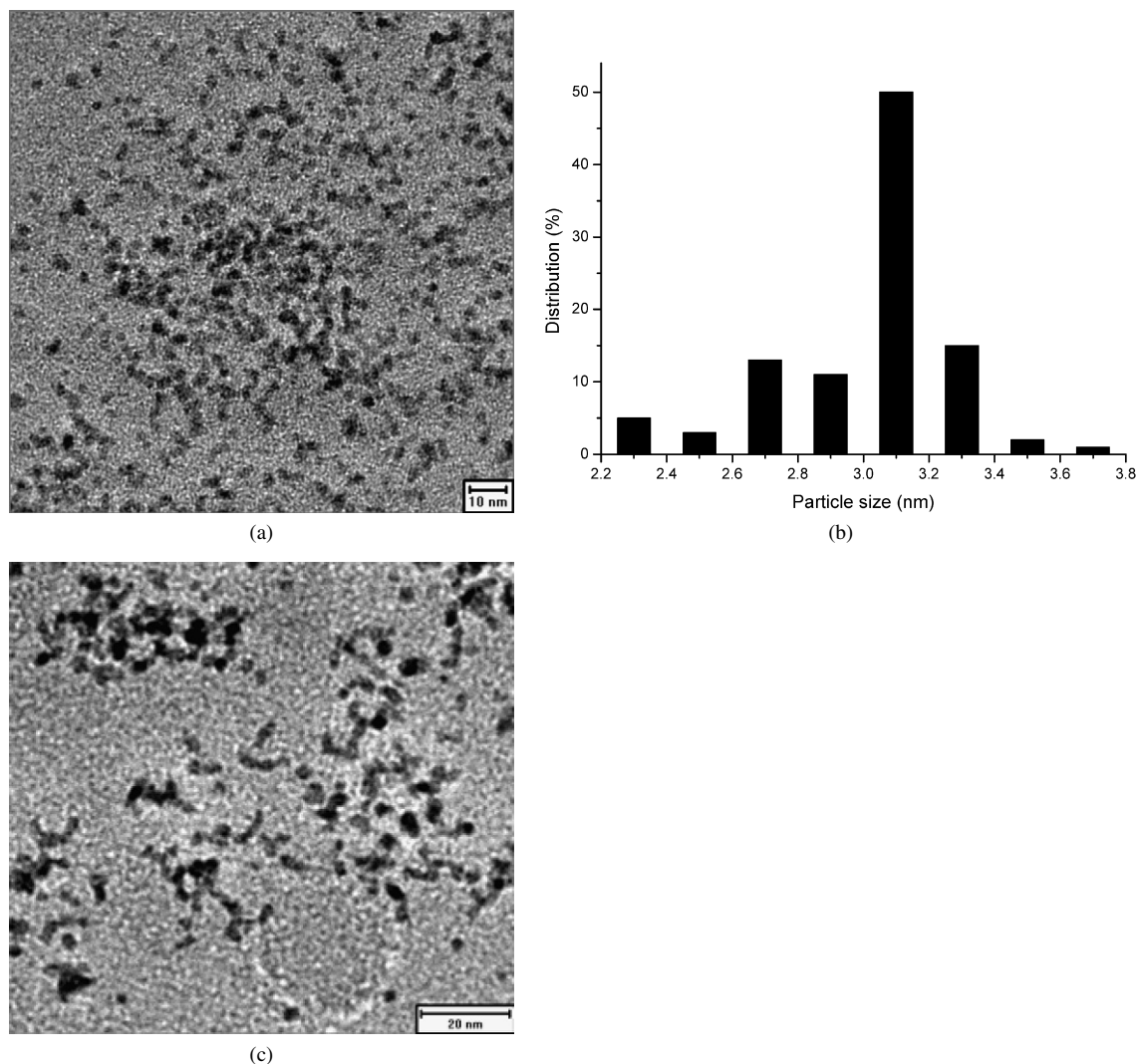


Fig. 3. (a) TEM micrograph of rhodium nanoparticles protected by ionic copolymer (from entry 3 in Table 2) in [BMIM][BF₄] before catalysis (scale bar = 10 nm). (b) Histogram showing the particle size distribution. (c) TEM micrograph of rhodium nanoparticles protected by ionic copolymer in [BMIM][BF₄] after hydrogenation of *p*-xylene (scale bar = 20 nm).

(M_n) was approximately 100,000, and the NVP concentration was ca. 57 mol% in the copolymers. RhCl₃ was reduced in 30 min at 60 °C in the presence of the IL-like copolymers but could not be reduced even at 75 °C for several hours in the presence of homopolymer, indicating the superior stabilization effect of IL-like copolymer compared with the simple homopolymer.

The effect of two IL-like copolymer stabilizers on the rhodium nanoparticles was compared in the hydrogenation of benzene in [BMIM][BF₄] under the same conditions (75 °C, 40 bar H₂, for 10 h). Conversions of 46% with a TOF of 115 h⁻¹ and 99% with a TOF of 243 h⁻¹ were obtained using the poly[NVP-*co*-VBIM]Br- and poly[NVP-*co*-VBIM]Cl-stabilized nanoparticles, respectively. This difference in activity is almost certainly due to the poisoning effect of the Br⁻ anions on nanoparticles, which, as noted elsewhere [38], leads to reduced catalytic activity.

The copolymer metal ratio also affected the ability of the rhodium nanoparticles to catalyze the hydrogenation reaction

(see Figs. S5 and S6 in supporting information). Benzene was hydrogenated in [BMIM][BF₄] containing Rh nanoparticles stabilized by various ratios of poly[NVP-*co*-VBIM]Cl and an optimized [copolymer]/[Rh] ratio of 5:1 mol/mol afforded rhodium nanoparticles that achieved a TTO of 20,000 with a TOF of 250 h⁻¹. In contrast, a [copolymer]/[Rh] ratio of 1:1 mol/mol afforded nanoparticle catalysts that maintained activity for only 15 min with a very low TOF of ca. 5 h⁻¹. Moreover, the catalytic activity of the Rh nanoparticles decreased by 20% when the [copolymer]/[Rh] was raised to 10:1 mol/mol, reflecting the need for an optimum balance between the stability and activity of the nanocatalyst. Rhodium aggregates prepared in the absence of a copolymer additive showed no activity in the reduction of benzene.

The polydispersity of the three poly(NVP-*co*-VBIM)Cl copolymers with different molecular weights [weight-average molecular weight (M_w)/numeral-average molecular weight (M_n)] ranged from 1.20 to 1.49 (Table 2). All of the copolymers effectively stabilized the nanoparticles in the hydrogenation of

Table 3
Infrared data of carbon monoxide adsorbed on IL-like copolymer^a stabilized rhodium nanoparticles before and after catalysis in [BMIM][BF₄]

Entry	Rhodium nanoparticles	Terminal CO $\nu_{\text{C=O}}$ (cm ⁻¹)	Bridged CO $\nu_{\text{C=O}}$ (cm ⁻¹)	T/B ^b
1	Fresh	2115	1819	1.95
2	After hydrogenation of <i>m</i> -xylene	2115	1817	1.66
3	After hydrogenation of <i>p</i> -xylene	2117	1817	1.81
4	After hydrogenation of isobutylbenzene	2119	1818	1.83
5 ^c	Deactivated (after hydrogenation of benzene—organic phase)	2121	1817	1.09
6 ^d	Deactivated (after hydrogenation of benzene—ionic liquid phase)	2119	1817	0.66

^a Poly(NVP-*co*-VBIMCl) ($M_n = 50,400$, $M_w = 75,300$), IL-copolymer/Rh = 5:1 (mol/mol).

^b Integration ratio of terminal per bridged adsorptions.

^c Upper layer of catalytic phase.

^d Lower layer of catalytic phase.

benzene and toluene with no appreciable differences in activity (see Table S7 and Fig. S4). The copolymer with $M_n = 50,400$ (entry 3 in Table 2) gave slightly higher conversions for benzene and toluene and thus were selected for evaluation in the hydrogenation of a range of arenes.

3.3. Characterization of the nanoparticle catalysts by TEM and FT-IR spectroscopic

The rhodium nanoparticles were analyzed by TEM and found to have a mean diameter of 3.0 nm and a standard deviation of 0.8 nm (Fig. 3). Because nanoparticle catalysts are usually not uniform, with the particles observed in the TEM representing only part of the system with respect to dispersity and size, the nanoparticles were studied in solution by infrared spectroscopy using CO as a probe.

As nanoparticles aggregate or increase in size, their surfaces undergo a change in geometry. Using CO as a probe, which coordinates with the vacant sites of the nanoparticles, allows tracking of such changes. IR spectra of CO chemisorbed on copolymer-stabilized rhodium nanoparticles in [BMIM][BF₄] (prepared by merely passing CO gas through the solution for 2 h) exhibited two main peaks centered at ca. 2115–2121 and 1817–1819 cm⁻¹ (see Table 3). The peaks in the range 2115–2121 cm⁻¹ can be assigned to terminally bound CO on the rhodium surface, and the peaks in the range 1817–1819 cm⁻¹ are characteristic of bridged CO ligands [39].

The relative ratio of terminal and bridged CO ligands on rhodium nanoparticles was estimated before and after catalysis to examine the potential coordination sites provided by the catalysts. We speculated that the rhodium catalysts were partially deactivated during the hydrogenation of *m*-xylene, *p*-xylene, and isobutylbenzene, because these substrates were converted

only in low yield. Completely deactivated catalysts were obtained from benzene hydrogenation after several runs, and particles from both the upper and lower phases were examined using the CO probe (Table 3, entries 5 and 6, respectively). Integration of terminal to bridged (T/B) adsorption was compared with fresh nanoparticle catalysts (Table 3, entry 1), the group of partially deactivated catalysts (Table 3, entries 2–4), and the completely deactivated catalysts (Table 3, entries 5 and 6). Table 3 clearly shows that the carbonyls bound to newly prepared rhodium nanoparticles had the highest terminal to bridged ratio of 1.95, which steadily decreased to 0.66, with the stepwise deactivation corresponding to a reduction in active reaction sites.

3.4. Mercury poisoning experiments

Mercury poisoning experiments are frequently performed to ascertain whether catalysts are truly homogeneous or heterogeneous (including soluble nanoparticle catalysts) [40]. Mercury poisoning experiments applied here revealed that hydrogen was no longer consumed after mercury was added to the reaction, demonstrating that the catalysts are heterogeneous (see Fig. S3).

4. Conclusion

Rhodium nanoparticles protected by IL-like copolymers are highly active catalysts for the hydrogenation of arenes. The nanoparticle catalysts protected by the IL-like copolymer [poly(NVP-*co*-VBIMCl)] immobilized in ILs can endure forcing reaction conditions, resulting in high reaction rates and high conversions. The solubility of the substrates in the reaction media and the steric/electronic properties of the substituents on the aromatic ring influence the rate of catalytic hydrogenation and the nature of the reaction product, that is, partially hydrogenated versus fully hydrogenated systems.

Our findings also demonstrate the delicate balance between activity and stability of IL-like stabilized nanoparticles. IR spectroscopy showed a strong correlation between the number of CO ligands chemisorbed on the rhodium nanoparticles and catalytic activity; that is, a decrease in ratio of the terminal to bridged adsorptions occurs as the catalyst is deactivated, which corresponds to a decrease in available reaction sites.

Acknowledgments

This work was supported by the National Science Foundation of China (projects nos. 20533010 and 20473002). The authors thank Professor Zi-Chen Li and Dr. Yong-Quan Dong, Department of Polymer Science and Engineering, College of Chemistry and Molecular Engineering, Peking University, for supplying the poly(NVP-*co*-VBIMCl) sample used in this study.

Supporting information

Supporting information for this article may be found on ScienceDirect, in the online version.

Please visit DOI: 10.1016/j.jcat.2007.05.014.

References

- [1] R.G. Finke, J.A. Widegren, *J. Mol. Catal. A Chem.* 191 (2003) 187.
- [2] D.B. Zhao, M. Wu, Y. Kou, E.Z. Min, *Catal. Today* 74 (2002) 157.
- [3] P. Wasserscheid, W. Keim, *Angew. Chem. Int. Ed.* 39 (2000) 3772.
- [4] J. Dupont, R.F. de Souza, P.A.Z. Suarez, *Chem. Rev.* 102 (2002) 3667.
- [5] J. Dupont, P.A.Z. Suarez, *Phys. Chem. Chem. Phys.* 8 (2006) 2441.
- [6] P. Migowski, J. Dupont, *Chem. Eur. J.* 13 (2007) 32.
- [7] J. Dupont, G.S. Fonseca, A.P. Umpierre, P.F.P. Fichtner, S.R. Teixeira, *J. Am. Chem. Soc.* 124 (2002) 4228.
- [8] L.S. Ott, R.G. Finke, *Inorg. Chem.* 45 (2006) 8382.
- [9] Y. Wang, N. Toshima, *J. Phys. Chem. B* 101 (1997) 5301.
- [10] K.S. Weddle, J.D. Aiken III, R.G. Finke, *J. Am. Chem. Soc.* 120 (1998) 5653.
- [11] J.D. Aiken, R.G. Finke, *J. Am. Chem. Soc.* 121 (1999) 8803.
- [12] X.D. Mu, J.Q. Meng, Z.C. Li, Y. Kou, *J. Am. Chem. Soc.* 127 (2005) 9694.
- [13] A. Stanislaus, B.H. Cooper, *Catal. Rev. Sci. Eng.* 36 (1994) 75.
- [14] P. Giannoccaro, M. Gargano, A. Fanizzi, C. Ferragina, M. Aresta, *Appl. Catal. A Gen.* 284 (2005) 77.
- [15] M.S. Eisen, T.J. Marks, *J. Am. Chem. Soc.* 114 (1992) 10358.
- [16] H. Gao, R.J. Angelici, *J. Am. Chem. Soc.* 119 (1997) 6937.
- [17] C. Bianchini, V. Dal Santo, A. Meli, S. Moneti, M. Moreno, W. Oberhauser, R. Psaro, L. Sordelli, F. Vizza, *Angew. Chem. Int. Ed.* 42 (2003) 2636.
- [18] K.H. Park, K. Jang, H.J. Kim, S.U. Son, *Angew. Chem. Int. Ed.* 46 (2007) 1152.
- [19] L.N. Lewis, *Chem. Rev.* 93 (1993) 2693.
- [20] J. Schulz, A. Roucoux, H. Patin, *Chem. Eur. J.* 6 (2000) 618.
- [21] C.M. Hagen, L. Vieille-Petit, G. Laurency, G. Süß-Fink, R.G. Finke, *Organometallics* 24 (2005) 1819.
- [22] L. Vieille-Petit, G. Süß-Fink, B. Therrien, T.R. Ward, H. Stoeckli-Evans, G. Labat, L. Karmazin-Brelot, A. Neels, T. Bürgi, R.G. Finke, C.M. Hagen, *Organometallics* 24 (2005) 6104.
- [23] T.J. Donohoe, R. Garg, C.A. Stevenson, *Tetrahedron: Asymmetry* 7 (1996) 317.
- [24] H. Nagahara, *Rev. J. Surf. Sci. Technol. Avant-Garde* 30 (1992) 951.
- [25] X.D. Mu, D.G. Evans, Y. Kou, *Catal. Lett.* 97 (2004) 151.
- [26] B.R. James, Y. Wang, T.Q. Hu, *Chem. Ind.* 68 (1996) 423.
- [27] L. Petrus, M.A. Noordermeer, *Green Chem.* 8 (2006) 861.
- [28] P.J. Dyson, *Dalton Trans.* (2003) 2964.
- [29] J.A. Widegren, R.G. Finke, *Inorg. Chem.* 41 (2002) 1558.
- [30] J. Blum, I. Amer, K.P.C. Vollhardt, H. Schwartz, G. Hohne, *J. Org. Synth.* 52 (1987) 2804.
- [31] Y. Chauvin, L. Missmann, H. Olivier, *Angew. Chem. Int. Ed. Engl.* 34 (1996) 2698.
- [32] P.A.Z. Suarez, J.E.L. Dullius, S. Einloft, R.F. de Souza, J. Dupont, *Inorg. Chim. Acta* 255 (1997) 207.
- [33] D. Zhao, P.J. Dyson, G. Laurency, J.S. McIndoe, *J. Mol. Catal. A Chem.* 214 (2004) 19.
- [34] P.J. Dyson, *Appl. Organomet. Chem.* 16 (2002) 495.
- [35] J.B. Ning, J. Xu, J. Liu, F. Lu, *Catal. Lett.* 109 (2006) 175.
- [36] G.S. Fonseca, A.P. Umpierre, P.F.P. Fichtner, S.R. Teixeira, J. Dupont, *Chem. Eur. J.* 9 (2003) 3263.
- [37] P.J. Dyson, G. Laurency, C.A. Ohlin, J. Vallance, T. Welton, *Chem. Commun.* (2003) 2418.
- [38] J.D. Aiken III, Y. Lin, R.G. Finke, *J. Mol. Catal. A Chem.* 114 (1996) 29.
- [39] A. Duteil, R. Quéau, B. Chaudret, *Chem. Mater.* 5 (1993) 341.
- [40] J.A. Widegren, M.A. Bennett, R.G. Finke, *J. Am. Chem. Soc.* 125 (2003) 10301.